

Quadrilateral and Hexahedral Mesh Generation based on Computational Conformal Geometry

David Xianfeng Gu^{1,2}

¹Department of Computer Science
Department of Applied Mathematics
State University of New York at Stony Brook

²Center of Mathematical Sciences and Applications
Harvard University

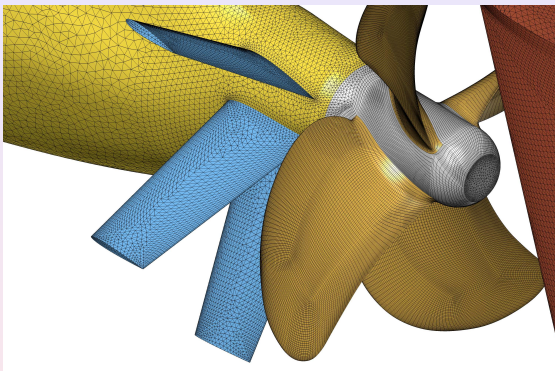
Workshop on Geometric Methods for Analyzing Discrete
Shapes, Davis, CA

Thanks for the invitation!

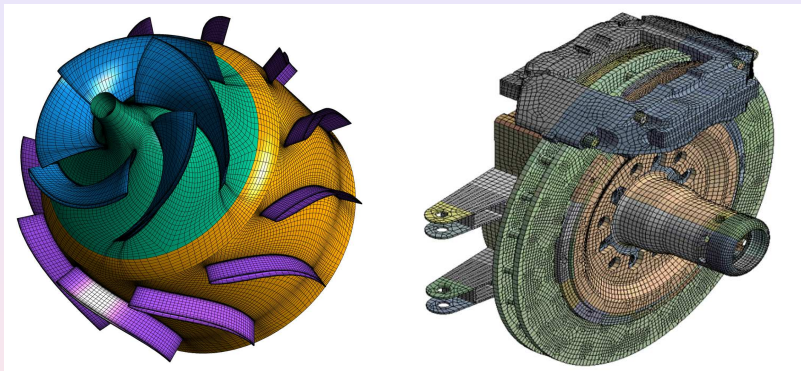
Thanks

This work is collaborated with Na Lei, Zhongxuan Luo, Xiaopeng Zheng, Wei Chen, Hang Si, Feng Luo and Xianfeng Gu, and many other mathematicians and computer scientists.

Motivation



Triangle meshes and quadrilateral meshes have been widely used in CAD and simulation.



Comparing to triangle meshes, quadrilateral meshes have many advantages.

Advantages of Quad-mesh

- Quad-mesh can better capture the local principle curvature directions or sharp features, as well as the semantics of modeled objects, therefore it is widely used in animation industry.
- Quad-mesh has tensor product structure, it is suitable for fitting splines or NURBS. Therefore it is applied for high-order surface modeling, such as CAD/CAM for Splines and NURBS, and the entertainment industry for subdivision surfaces.
- Patches of semi-regular quad meshes with a rectangular grid topology, naturally match the sampling pattern of textures. Therefore quad-mesh is highly preferred for texturing and compression.

Categories of Quad-meshes

- 1 **Regular quad-mesh:** all the interior vertices are with topological valence 4, there are no singularities, such as geometry image.
- 2 **Semi-regular quad-mesh:** The separatrices divide the quad-mesh into several topological rectangles, the interior of each topological rectangle is regular grids.
- 3 **Valence semi-regular quad-mesh:** The number of singularities are few, but the separatrices have complicated global behavior, they may have intersections, form spirals and go through most edges.
- 4 **Unstructured quad-mesh:** A large fraction of its vertices are irregular.

Regular vs Semi-regular Quad-mesh

- Regular quad-meshes have strong topological requirements for the surfaces, such as topological torus or annulus.
- Semi-regular quad-meshes can be realized for surfaces with any topologies, but the number of singularities, the behavior of separatrices are difficult to control.

We propose **generalized regular quad-mesh**, which is between the regular and semi-regular categories, combines their advantages and overcomes their disadvantages.

- 1 Comparing with regular quad-meshes, ours have no restriction on topologies;
- 2 Comparing with semi-regular quad-meshes, ours minimizes the number of singularities, simplifies the global behavior of separatrices. Namely, it is more regular.

main contributions

- 1 Propose the generalized regular quad-mesh, it can be applied for surfaces with general topologies and with higher regularity.
- 2 It reduces the number of singularities to the theoretic lower bound and simplifies the global behavior of separatrices.
- 3 It is with C^∞ smoothness except the singular vertices and global tensor product structure, suitable for spline fitting application.
- 4 The method is based on surface foliation theory and gives the complete solutions, which form a $6g - 6$ linear space.
- 5 The algorithm can be fully automatic without any user input or intervention.

Previous Works

Theorem (Thurston 93 and Mitchell 96)

For a genus zero closed surface, a quadrilateral mesh admits a hexahedral mesh of the enclosed volume if and only if it has even number of cells.

- W. Thurston, Hexahedral decomposition of polyhedra, posting to Sci.Math. (25 October 1993).
- S. A. Mitchell, A characterization of the quadrilateral meshes of a surface which admit a compatible hexahedral mesh of the enclosed volume, proceeding of STACS 96, pp. 465 – 476.

Theorem (Mitchell 96)

For a genus g closed surface in \mathbb{R}^3 , with a quad-mesh,

- 1 A compatible hex-mesh exists if one can find g disjoint topological disks in the interior body, each bounded by an cycle of even length in the quad-mesh, that cut the interior body into a ball.*
- 2 A compatible hex-mesh does not exist if there is a topological disk in the interior whose boundary is a cycle of odd length in the quad-mesh.*

- S. A. Mitchell, A characterization of the quadrilateral meshes of a surface which admit a compatible hexahedral mesh of the enclosed volume, proceeding of STACS 96, pp. 465 – 476.

Theorem (Erickson 2014)

Let Ω be a compact connected subset of \mathbb{R}^3 whose boundary $\partial\Omega$ is a (possibly disconnected) 2-manifold, and let \mathcal{Q} be a topological quad-mesh on $\partial\Omega$ with an even number of facets. The following conditions are equivalent:

- 1 \mathcal{Q} is the boundary of a topological hex-mesh of Ω .*
 - 2 Every subgraph of \mathcal{Q} that is null-homologous in Ω has an even number of edges.*
 - 3 The dual of \mathcal{Q} is null-homologous in Ω .*
- J. Erickson, Efficiently Hex-Meshing Things with Topology, Discrete and Computational Geometry 52(3):427-449,2014.

Generalization of Thurston and Mitchell's works.

These theoretic works consider general unstructured hex-meshes, which do not have local tensor product structure, therefore can not be applied for Mesh-TSpline conversion.

The “Frame field” method constructs smooth frame field, the hex-mesh is extracted from the field.

- 1 J. Huang, Y. Tong, H. Wei, H. Bao, Boundary aligned smooth 3d cross- frame field, ACM Trans. Graph. 30 (6) (2011) 143.
- 2 Y. Li, Y. Liu, W. Xu, W. Wang, B. Guo, All-hex meshing using singularity-restricted field, ACM Trans. Graph. 31 (6) (2012).
- 3 M. Nieser, U. Reitebuch, K. Polthier, Cubecover-parameterization of 3d volumes, Comput. Graph. Forum 30(5) (2011), 1397 – 1406.

The automatic generation of frame fields with prescribed singularity structure is unsolved.

The “advancing front” approach generates a hex-mesh from the boundary of the surface mesh inward.

- 1 Pastering method: T. D. Blacker, R. J. Meyers, Seams and wedges in plastering: A 3d hexahedral mesh generation algorithm, *Engineering with Computers* 9(2) (1993) 83 – 93.
- 2 Harmonic Field method: M. Li, R. Tong, All-hexahedral mesh generation via inside-out advancing front based on harmonic fields, *The Visual Computer* 28(6) (2012) 839 – 847.

The singularities might be propagated to the medial axes, which might lead to non-hexahedron shaped elements.

The “advancing front” approach generates a hex-mesh from the boundary of the surface mesh inward, whisker weaving method.

- 1 T. J. Tautges, T. Blacker, S. A. Mitchell, The whisker weaving algorithm: A connectivitybased method for constructing all-hexahedral finite element meshes (1995).
- 2 F. Ledoux, J.-C. Weill, An extension of the reliable whisker weaving algorithm, in: 16th International Meshing Roundtable, 2007.

The hex-mesh has no local tensor product structure.

Theoretic Foundation

Riemann Surface Theory

Riemann Surface

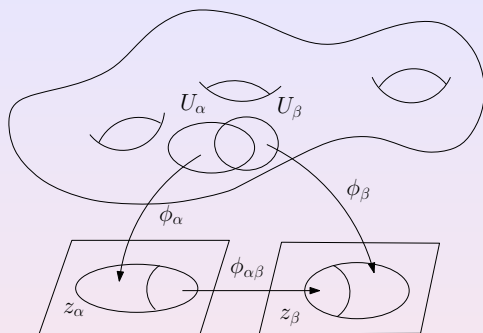


Figure: Riemann Surface.

A surface is covered by a complex atlas \mathcal{A} , such that all chart transitions are bi-holomorphic. $\phi_{\alpha\beta} : (x, y) \mapsto (u, v)$ satisfies Cauchy-Riemann equation:

$$u_x = v_y, \quad u_y = -v_x,$$

Definition (Meromorphic Function)

Suppose $f : M \rightarrow \mathbb{C} \cup \{\infty\}$ is a complex function defined on the Riemann surface M . If for each point $p \in M$, there is a neighborhood $U(p)$ of p with local parameter $z(p) = 0$, f has Laurent expansion

$$f(z) = \sum_{i=k}^{\infty} a_i z^i,$$

then f is called a meromorphic function.

Definition (Meromorphic Differential)

Given a Riemann surface $(M, \{z_\alpha\})$, ω is a meromorphic differential of order n , if it has local representation,

$$\omega = f_\alpha(z_\alpha)(dz_\alpha)^n,$$

where $f_\alpha(z_\alpha)$ is a meromorphic function, n is an integer; if $f_\alpha(z_\alpha)$ is a holomorphic function, then ω is called a holomorphic differential of order n .

Definition (Zeros and Poles)

Suppose $f : M \rightarrow \mathbb{C} \cup \{\infty\}$ is a meromorphic function. For each point p , there is a neighborhood $U(p)$ of p with local parameter $z(p) = 0$, f has Laurent expansion

$$f(z) = \sum_{i=k}^{\infty} a_i z^i,$$

if $k > 0$, then p is a zero with order k ; if $k = 0$, then p is a regular point; if $k < 0$, then p is a pole with order k . The assignment of p with respect to f is denoted as $v_p(f) = k$.

The zeros and poles of a meromorphic differential are defined in the similar way.

Definition (Divisor)

The Abelian group freely generated by points on a Riemann surface is called the divisor group, every element is called a divisor, which has the form $D = \sum_p n_p p$. The degree of a divisor is defined as $\deg(D) = \sum_p n_p$. Suppose $D_1 = \sum_p n_p p$, $D_2 = \sum_p m_p p$, then $D_1 \pm D_2 = \sum_p (n_p \pm m_p) p$; $D_1 \leq D_2$ if and only if for all p , $n_p \leq m_p$.

Definition (Meromorphic Function Divisor)

Given a meromorphic function f defined on a Riemann surface S , its divisor is defined as $(f) = \sum_p v_p(f) p$, where $v_p(f)$ is the assignment of p with respect to f .

The divisor of a meromorphic function is called a principle divisor. The divisor of a meromorphic differential is defined in the similar way.

Theorem

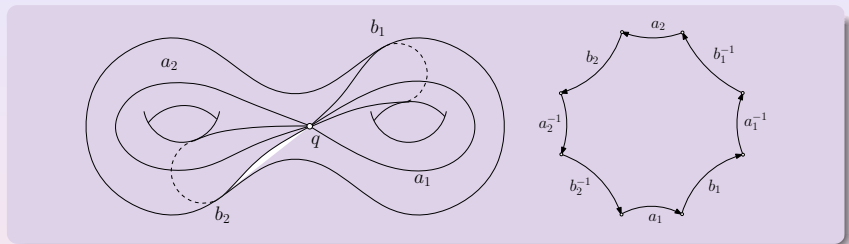
Suppose M is a compact Riemann surface with genus g , f is a meromorphic function, then

$$\deg((f)) = 0,$$

ω is a meromorphic differential, then

$$\deg((\omega)) = 2g - 2.$$

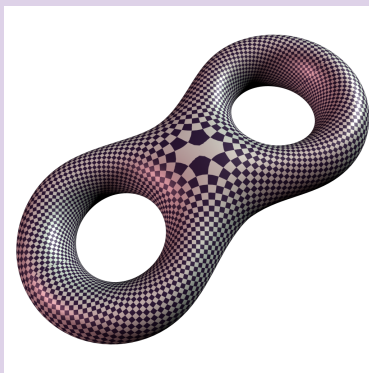
Canonical Fundamental Group Generators



Algebraic intersection numbers satisfy the conditions:

$$a_i \cdot b_j = \delta_{ij}, a_i \cdot a_j = 0, b_i \cdot b_j = 0.$$

Holomorphic Differential Group Basis



The holomorphic one-form basis $\{\varphi_1, \varphi_2, \dots, \varphi_g\}$ satisfy the dual condition

$$\int_{a_j} \varphi_i = \delta_{ij}.$$

Definition (Period Matrix)

Suppose M is a compact Riemann surface of genus g , with canonical fundamental group basis

$$\{a_1, a_2, \dots, a_g, b_1, b_2, \dots, b_g\}$$

and holomorphic one form basis

$$\{\varphi_1, \varphi_2, \dots, \varphi_g\}$$

The period matrix is defined as $[A, B]$

$$A = \left(\int_{a_j} \varphi_i \right), B = \left(\int_{b_j} \varphi_i \right).$$

Matrix B is symmetric, $\text{Im}g(B)$ is positive definite.

Definition (Jacobi Variety)

Suppose the period matrix

$$A = (A_1, A_2, \dots, A_g), \quad B = (B_1, B_2, \dots, B_g),$$

the lattice Γ is

$$\Gamma = \left\{ \sum_{i=1}^g \alpha_i A_i + \sum_{j=1}^g \beta_j B_j \right\},$$

the Jacobi variety of M is defined as

$$J(M) = \mathbb{C}^g / \Gamma.$$

Definition (Jacobi Map)

Given a compact Riemann surface M , choose a set of canonical fundamental group generators $\{a_1, \dots, a_g, b_1, \dots, b_g\}$, and obtain a fundamental domain Ω ,

$$\partial\Omega = a_1 b_1 a_1^{-1} b_1^{-1} a_2 b_2 a_2^{-1} b_2^{-1} \cdots a_g b_g a_g^{-1} b_g^{-1}.$$

choose a base point p_0 , the Jacobi map $\mu : M \rightarrow J(M)$ is defined as follows: for any point $p \in M$, choose a path γ from p_0 to p inside Ω ,

$$\mu(p) = \left(\int_{\gamma} \varphi_1, \int_{\gamma} \varphi_2, \dots, \int_{\gamma} \varphi_g \right)^T.$$

Theorem (Abel)

Suppose M is a compact Riemann surface with genus g , D is a divisor, $\deg(D) = 0$. D is principle if and only if

$$\mu(D) = 0 \quad \text{in } J(M).$$

Theory: measured foliation

Measured Foliation



Figure: A finite measured foliation on a genus two surface.

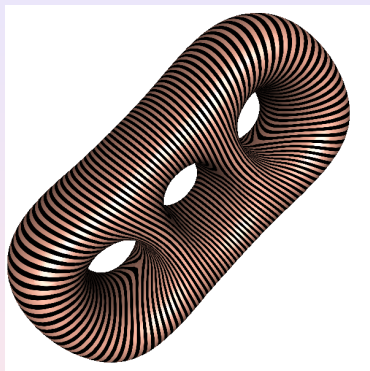


Figure: A finite measured foliation on a genus three surface.

Definition (Measured Foliation)

Let S be a compact Riemann surface of genus $g > 1$. A C^k measured foliation on S with singularities z_1, \dots, z_l of order k_1, \dots, k_l respectively is given by an open covering $\{U_i\}$ of $S - \{z_1, \dots, z_l\}$ and open sets V_1, \dots, V_l around z_1, \dots, z_l respectively along with C^k real valued functions v_i defined on U_i s.t.

- 1 $|dv_i| = |dv_j|$ on $U_i \cap U_j$
- 2 $|dv_i| = |\operatorname{Im}(z - z_j)^{k_j/2} dz|$ on $U_i \cap V_j$.

The kernels $\ker dv_i$ define a C^{k-1} line field on S which integrates to give a foliation \mathcal{F} on $S - \{z_1, \dots, z_l\}$, with $k_j + 2$ pronged singularity at z_j . Moreover, given an arc $\gamma \subset S$, we have a well-defined measure $\mu(\gamma)$ given by $\mu(\gamma) = |\int_\gamma dv|$, where $|dv|$ is defined by $|dv|_{U_i} = |dv_i|$.

Measured Foliation



Figure: Finite measured foliations on a genus three surface.

Measured Foliation

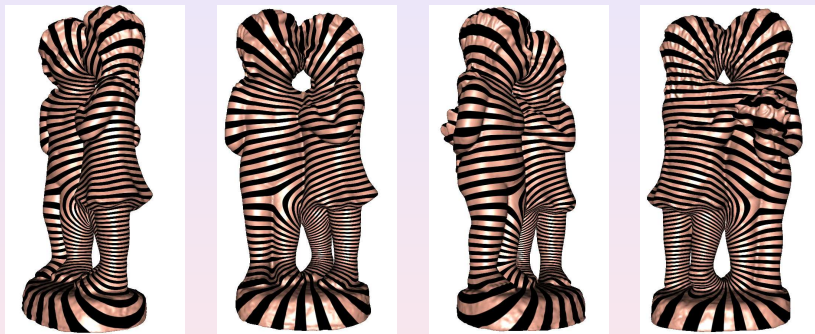


Figure: Holomorphic quadratic differentials on a genus three surface.

Whitehead Move

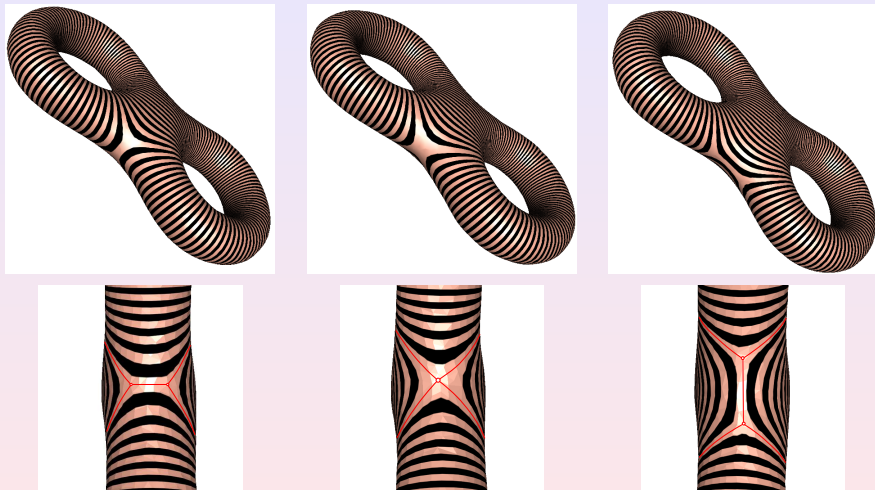


Figure: Equivalent measured foliations and Whitehead moves.

Two measured foliations (\mathcal{F}, μ) and (\mathcal{G}, ν) are said to be equivalent if after some Whitehead moves on \mathcal{F} and \mathcal{G} , there is a self-homeomorphism of S which takes \mathcal{F} to \mathcal{G} , and μ to ν . Here a Whitehead move is the transformation of one foliation to another by collapsing a finite arc of a leaf between two singularities, or the inverse procedure.

Theory: Strebel Differential

Holomorphic Quadratic Differentials

Definition (Holomorphic Quadratic Differentials)

Suppose S is a Riemann surface. Let Φ be a complex differential form, such that on each local chart with the local complex parameter $\{z_\alpha\}$,

$$\Phi = \varphi_\alpha(z_\alpha) dz_\alpha^2,$$

where $\varphi_\alpha(z_\alpha)$ is a holomorphic function.

- A holomorphic quadratic differential on a genus zero closed surface must be 0.
- The linear space of all holomorphic quadratic differentials is 1 complex dimensional, where the genus $g = 1$.
- The linear space of all holomorphic quadratic differentials is $3g - 3$ complex dimensional, where the genus $g > 1$.

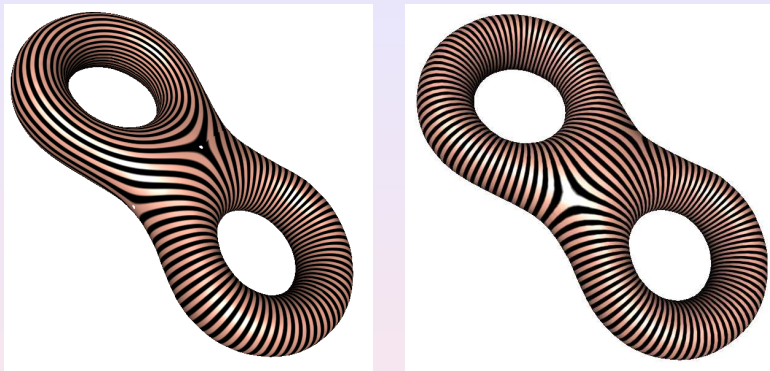


Figure: Holomorphic quadratic forms on the genus two surface.

Definition (Zeros)

A point $z_i \in S$ is called a *zero* of Φ , if $\varphi(z_i)$ vanishes. A holomorphic quadratic differential has $4g - 4$ zeros.

Definition (Natural Coordinates)

For any point away from zero, we can define a local coordinates

$$\zeta(p) := \int^p \sqrt{\varphi(z)} dz. \quad (1)$$

which is the so-called *natural coordinates* induced by Φ .

The curves with constant real natural coordinates are called the *vertical trajectories*, with constant imaginary natural coordinates *horizontal trajectories*. The trajectories through the zeros are called the *critical trajectories*.

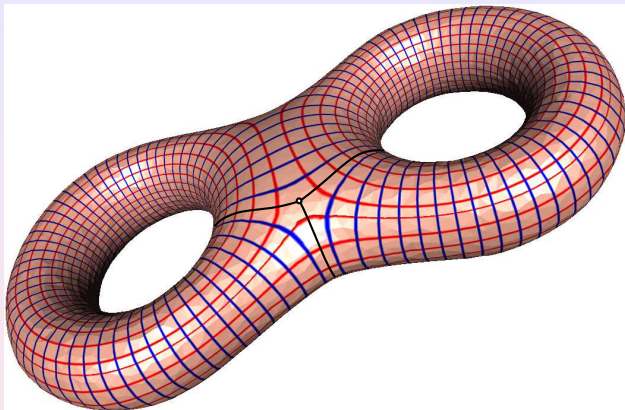
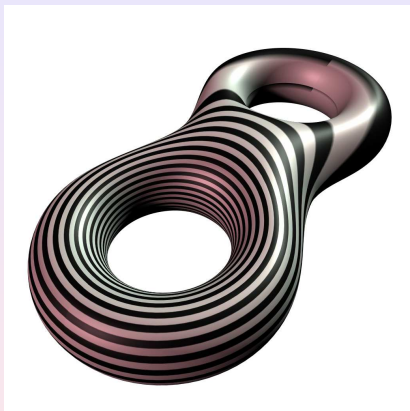


Figure: Trajectories of a holomorphic quadratic differential, blue - horizontal, red - vertical, black - critical trajectory.

Strebel Differential



(a) non-Strebel



(b) Strebel

Figure: A non-Strebel (a) and a Strebel differential (b).

Definition (Strebel)

Given a holomorphic quadratic differential Φ on a Riemann surface S , if all of its horizontal trajectories are finite, then Φ is called a Strebel differential.

A holomorphic quadratic differential Φ is Strebel, if and only if its critical horizontal trajectories form a finite graph. The horizontal trajectories of a holomorphic differential may be infinite spirals as in the left frame, or finite loops as in the right frame.

From Differential to Foliation

Given a holomorphic quadratic differential Φ on a Riemann surface S , it defines a measured foliation in the following way: Φ induces the natural coordinates ζ , the local measured foliations are given by

$$(\{\operatorname{Im}\zeta = \text{const}\}, |d\operatorname{Im}\zeta|), \quad (2)$$

then piece together to form a measured foliation known as the *horizontal measured foliation* of Φ . Similarly, the vertical measured foliation of Φ is given by

$$(\{\operatorname{Re}\zeta = \text{const}\}, |d\operatorname{Re}\zeta|). \quad (3)$$

From Foliation to Differential

Hubbard and Masur proved the following fundamental theorem connecting measured foliation and holomorphic quadratic differentials.

Theorem (Hubbard-Masur)

If (\mathcal{F}, μ) is a measured foliation on a compact Riemann surface S , then there is a unique holomorphic quadratic differential Φ on S whose horizontal foliation is equivalent to (\mathcal{F}, μ) .

Quad-Mesh/Hex-Mesh Theorems

Metric Holonomy Condition

Quad-Mesh

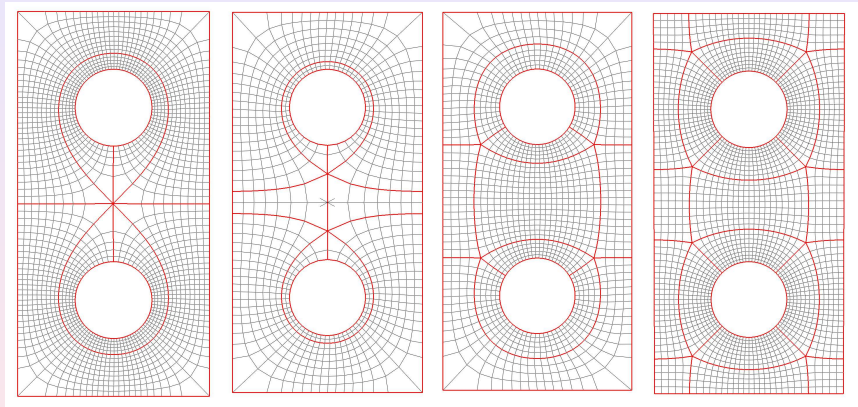


Figure: Quad-meshes with different number of singularities.

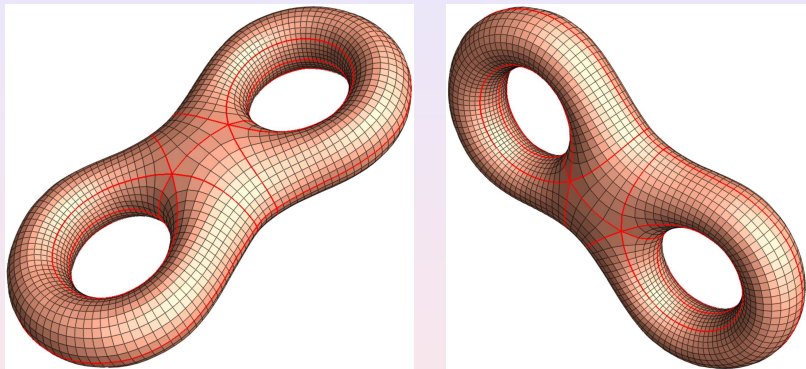


Figure: Quad-meshes with different number of singularities.

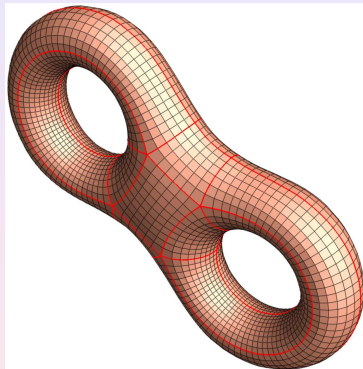
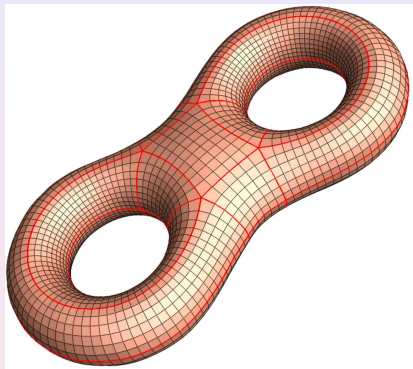


Figure: Quad-meshes with different number of singularities.

Definition (Quad-Metric)

Given a quad-mesh \mathcal{Q} , each face is treated as the unit planar square, this will define a Riemannian metric, the so-called quad-mesh metric $\mathbf{g}_{\mathcal{Q}}$, which is a flat metric with cone singularities.

Theorem (Quad-Mesh Metric Conditions)

Given a quad-mesh \mathcal{Q} , the induced quad-mesh metric is $\mathbf{g}_{\mathcal{Q}}$, which satisfies the following four conditions:

- 1 *Gauss-Bonnet condition;*
- 2 *Holonomy condition;*
- 3 *Boundary Alignment condition;*
- 4 *Finite geodesic lamination condition.*

Gauss-Bonnet Condition

Definition (Curvature)

Given a quad-mesh \mathcal{Q} , for each vertex v_i , the curvature is defined as

$$K(v) = \begin{cases} \frac{\pi}{2}(4 - k(v)) & v \notin \partial\mathcal{Q} \\ \frac{\pi}{2}(2 - k(v)) & v \in \partial\mathcal{Q} \end{cases}$$

where $k(v)$ is the topological valence of v , i.e. the number of faces adjacent to v .

Theorem (Gauss-Bonnet)

Given a quad-mesh \mathcal{Q} , the induced metric is $\mathbf{g}_{\mathcal{Q}}$, the total curvature satisfies

$$\sum_{v_i \in \partial\mathcal{Q}} K(v_i) + \sum_{v_i \notin \partial\mathcal{Q}} K(v_i) = 2\pi\chi(\mathcal{Q}).$$

Namely

Definition (Holonomy)

Given a quad-mesh \mathcal{Q} , the induced flat metric is $\mathbf{g}_{\mathcal{Q}}$, the set of singular vertices is $\mathcal{S}_{\mathcal{Q}}$. Suppose $\gamma: [0, 1] \rightarrow \mathcal{Q} \setminus \mathcal{S}_{\mathcal{Q}}$ is a closed loop not through singularities, choose a tangent vector $\mathbf{v}(0) \in T_{\gamma(0)}\mathcal{Q}$, parallel transport $\mathbf{v}(0)$ along $\gamma(t)$ to obtain $\mathbf{v}(1)$. The rotation angle from $\mathbf{v}(0)$ to $\mathbf{v}(1)$ in $T_{\gamma(0)}\mathcal{Q}$ is the holonomy of γ , denoted as $\rho(\gamma)$.

Because $\mathbf{g}_{\mathcal{Q}}$ is flat on $\mathcal{Q} \setminus \mathcal{S}_{\mathcal{Q}}$, if γ_1 is homotopic to γ_2 , then $\rho(\gamma_1) = \rho(\gamma_2)$. Therefore, holonomy is a homomorphism from the fundamental group to \mathbb{S}^1 ,

$$\lambda: \pi_1(\mathcal{Q} \setminus \mathcal{S}_{\mathcal{Q}}) \rightarrow \mathbb{S}^1.$$

Face Loop

Definition (face path)

A sequence of faces, $\{f_0, f_1, \dots, f_n\}$, such that f_i and f_{i+1} share an edge. If f_0 equals to f_n , then the face path is called a face loop.

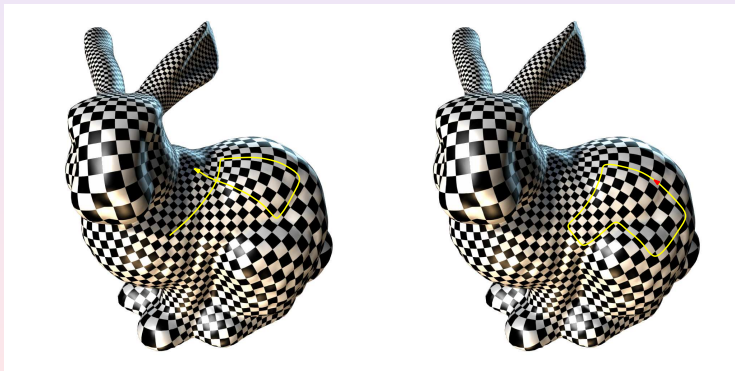


Figure: A face path and a face loop.

Fundamental Group

Definition (Fundamental Group)

Given a quad-mesh \mathcal{Q} with singularities $S_{\mathcal{Q}}$, fix a base face σ_0 , the homotopy classes of face loops through σ_0 form the fundamental group, denoted as $\pi_1(\mathcal{Q} - S_{\mathcal{Q}}, \sigma_0)$.

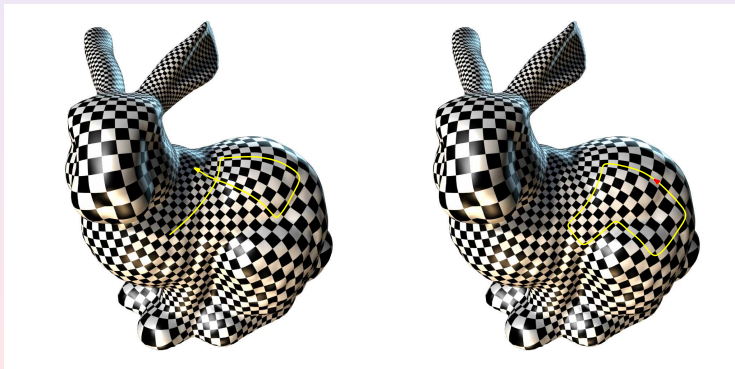
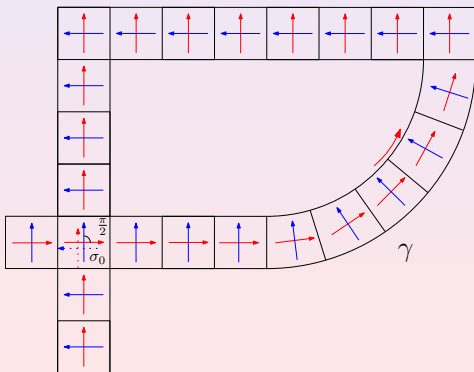


Figure: A face path and a face loop.

Holonomy

Definition (Holonomy of a loop)

Given a face loop γ through σ_0 , fix a frame on σ_0 , parallel transport the frame along γ . When we return to σ_0 , the frame is rotated by an angle $k\pi/2$, which is called the holonomy of γ , and denoted as $\langle \gamma \rangle$.



Theorem (Holonomy)

Given a quad-mesh \mathcal{Q} with induced metric $\mathbf{g}_{\mathcal{Q}}$, the holonomy homomorphism is

$$\lambda : \pi_1(\mathcal{Q} \setminus \mathcal{S}_{\mathcal{Q}}) \rightarrow \mathbb{S}^1,$$

then the holonomy group is a subgroup of rotation group

$$\lambda(\pi_1(\mathcal{Q} \setminus \mathcal{S}_{\mathcal{Q}})) \subset \mathcal{R} = \{e^{i\frac{k\pi}{2}}, k = 0, 1, 2, 3\}.$$

Boundary Alignment Condition

Given a flat cone metric with satisfying the holonomy condition, one can define a global cross field by parallel transportation, which gives the stream lines.

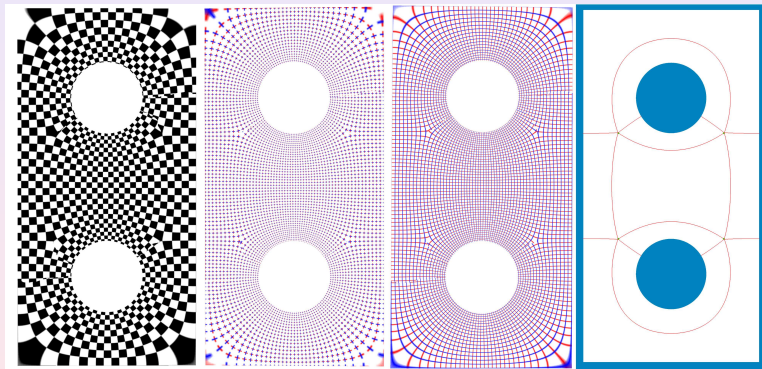


Figure: Quad-mesh with 4 saddle points.

Boundary Alignment Condition

Definition (Boundary Alignment Condition)

Given a quad-mesh \mathcal{Q} , with induced metric $\mathbf{g}_{\mathcal{Q}}$, one can define a global cross field by parallel transportation, which is aligned with the boundaries.

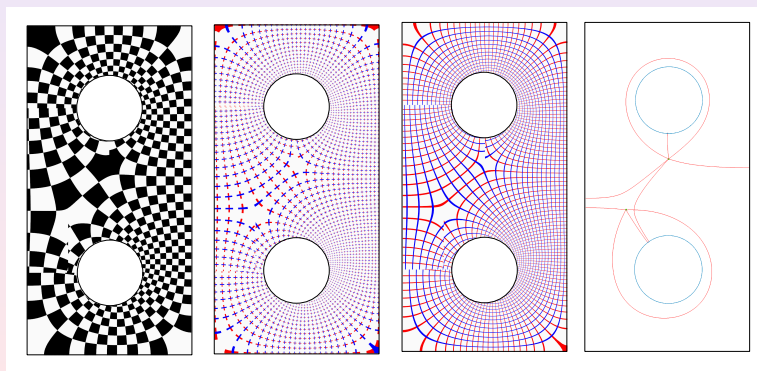


Figure: Cross field is mis-aligned with the inner boundaries. ▶

Finite Geodesic Lamination Condition

Definition (Finite Geodesic Lamination Condition)

The stream lines parallel to the cross field are finite geodesic loops. This is the finite geodesic lamination condition.

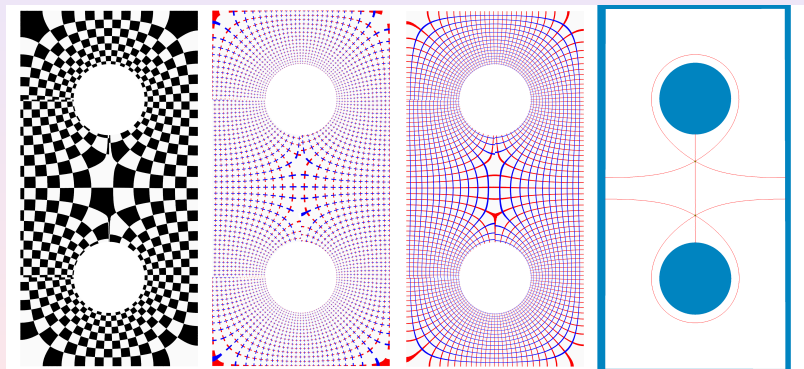
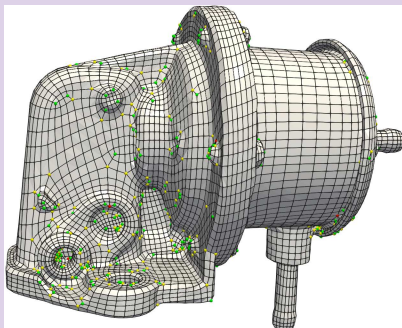
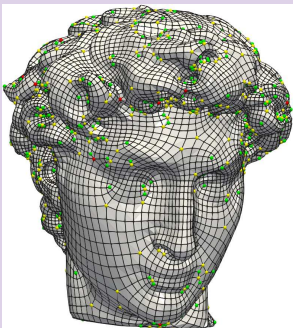


Figure: Finite geodesic lamination condition.

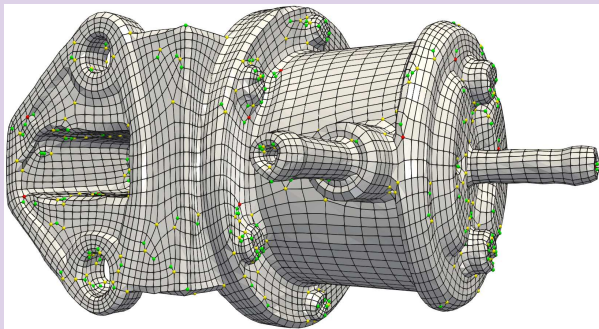
Quad-Mesh Singularity Abel condition

Singularities on Quadrilateral Meshes



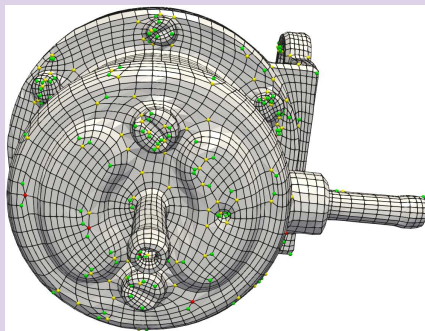
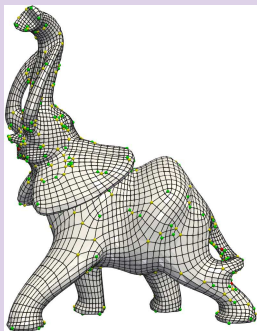
Yellow, Green and Red vertices are with topological valence 3, 5 and 6 respectively.

Singularities on Quadrilateral Meshes



Yellow, Green and Red vertices are with topological valence 3, 5 and 6 respectively.

Singularities on Quadrilateral Meshes



Yellow, Green and Red vertices are with topological valence 3, 5 and 6 respectively.

Quad-Mesh Riemannian Metric

Definition (Quad-Mesh Metric)

Suppose Q is a closed quadrilateral mesh, if each face is treated as a unit square, then Q induces a Riemannian metric \mathbf{g}_Q .

Theorem (Gauss-Bonnet)

Suppose Q is a closed quad-mesh, then

$$\sum_{v \in Q} (4 - k(v)) = 4\chi(M). \quad (4)$$

where v is a vertex of Q with valence $k(v)$.

Theorem (Holonomy Condition)

Suppose Q is a closed quad-mesh, then \mathbf{g}_Q induces holonomy group is a subgroup of the rotation group $\{e^{i\frac{k}{2}\pi}, k \in \mathbb{Z}\}$.



Definition (Divisor)

The Abelian group freely generated by points on a Riemann surface is called the divisor group, every element is called a divisor, which has the form $D = \sum_p n_p p$. The degree of a divisor is defined as $\deg(D) = \sum_p n_p$. Suppose $D_1 = \sum_p n_p p$, $D_2 = \sum_p m_p p$, then $D_1 \pm D_2 = \sum_p (n_p \pm m_p) p$; $D_1 \leq D_2$ if and only if for all p , $n_p \leq m_p$.

Definition (Quad-Mesh Divisor)

Suppose Q is a closed quadrilateral mesh, then Q induces a divisor

$$D_Q = \sum_{v_i \in Q} (k(v_i) - 4)v_i,$$

where v_i is a vertex with valence $k(v_i)$.

Central Question

Given a divisor D on a closed surface (M, \mathbf{g}) , whether there exists a quad-mesh Q on M , such that the metric induced by Q is conformal to \mathbf{g} , and the divisor of Q is D ?

From Gauss-Bonnet condition, we know a necessary condition of D should be

$$\deg(D) = -4\chi(M).$$

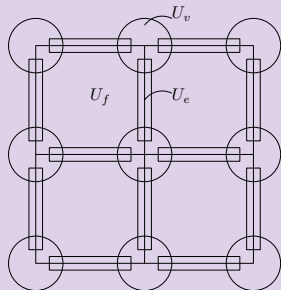
But only this condition can not guarantee the holonomy condition.

Quad-Mesh Riemann Surface

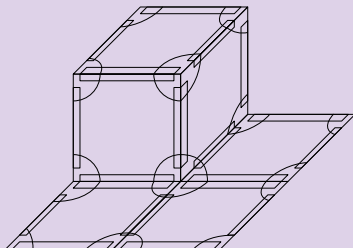
Theorem (Quad-Mesh Riemann Surface)

Suppose Q is a closed quadrilateral mesh, then Q induces a conformal structure and can be treated as a Riemann surface M_Q .

Proof.



(a) conformal atlas



(b) singularities

Quad-Mesh Meromorphic Differential

Theorem (Quad-Mesh Meromorphic Differential)

Suppose Q is a closed quadrilateral mesh, then Q induces meromorphic quartic differential.

Proof.

On each face f , define dz_f , $\omega_Q = (dz_f)^4$; vertex face transition

$$z_v^{\frac{k}{4}} = e^{i\frac{n\pi}{2}} z_f + \frac{1}{2}(\pm 1 \pm i) \quad (5)$$

where k is the vertex valence, therefore

$$\left(\frac{k}{4}\right)^4 z_v^{k-4} (dz_v)^4 = (dz_f)^4 = \omega_Q. \quad (6)$$



Theorem (Quad-Mesh Abel Condition)

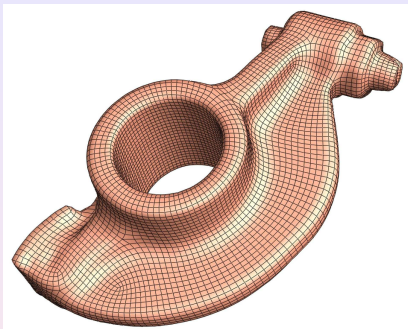
Suppose Q is a closed quadrilateral mesh, then for any holomorphic differential φ

$$\mu(D_Q - 4(\varphi)) = 0 \quad \text{in } J(M_Q). \quad (7)$$

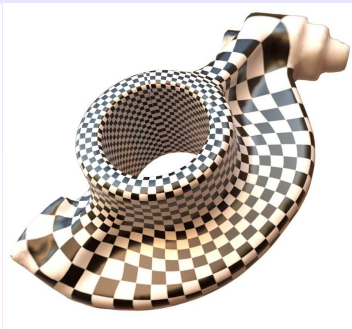
Theorem (Quartic Differential to Quad-Mesh)

Suppose M is a Riemann surface, ω is a meromorphic quartic differential with finite trajectories, then ω induces a quadrilateral mesh Q , such that the poles or zeros with order k of ω corresponds to the singular vertices of Q with valence $k + 4$.

Genus One Case



a) quad-mesh



b) holomorphic 1-form

The induced meromorphic quartic differential has 18 poles and 18 zeros.

$$D_Q = \sum_{i=1}^{18} (p_i - q_i),$$

The results of the Abel-Jacobi map are as follows:

$$\mu \left(\sum_{j=1}^{18} p_j \right) = 2.61069 + i0.588368,$$

and

$$\mu \left(\sum_{i=1}^{18} q_i \right) = 2.61062 + i0.588699.$$

Hence, $\mu(D_Q)$ is the difference between them, which equals to $6.967e-05 - i3.3064e-4$, very close to the origin in $J(S_Q)$.

Figure Eight Case

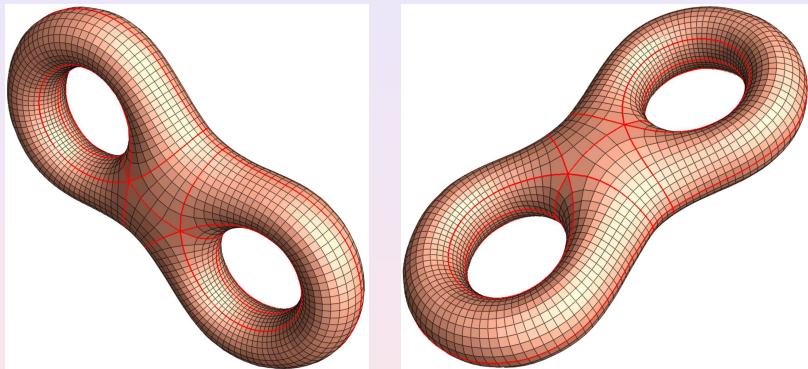


Figure: The input genus two quad-mesh.

Figure Eight Case



(a) tunnel loops



(b) handle loops

Figure: The homology group basis.

Figure Eight Case

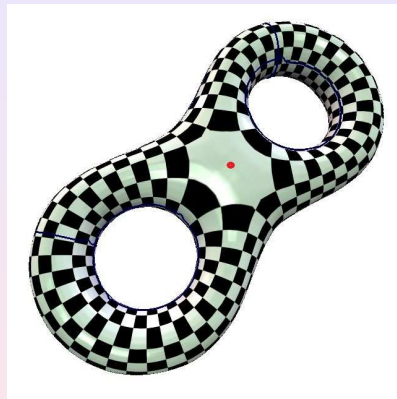
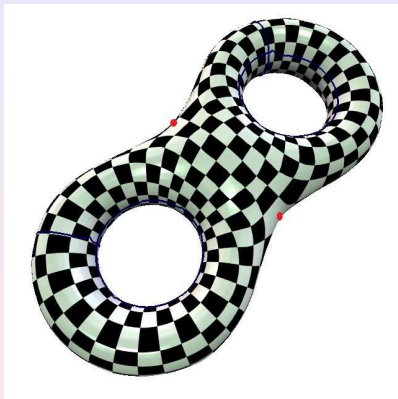


Figure: The holomorphic differential basis.

Abel Condition

We set φ_0 as ω_0 and verify the Abel-Jacobi condition by computing the Abel-Jacobi map $\mu(D_Q - 4(\omega_0))$. The period matrix A of the Riemann surface S_Q is

$$\begin{pmatrix} 0.99999999 - i1.4209e-09 & -0.99999989 + i6.01812e-08 \\ 0.99999998 + i5.12829e-09 & 0.99999992 - i2.88896e-08 \end{pmatrix}$$

The period matrix B is

$$\begin{pmatrix} 3.18e-08 + i0.38191542 & 4.7433845e-20 + i0.3861979 \\ 1.433e-08 + i0.44392235 & -2.3716923e-20 - i0.44820492 \end{pmatrix}$$

The Abel-Jacobi image of the divisor,

$$\mu(D_Q - 4(\omega_0)) = \begin{pmatrix} 1e-06 \\ 2e-07 - i1.6e-06 \end{pmatrix},$$

which is very close to 0.

Genus Two Case

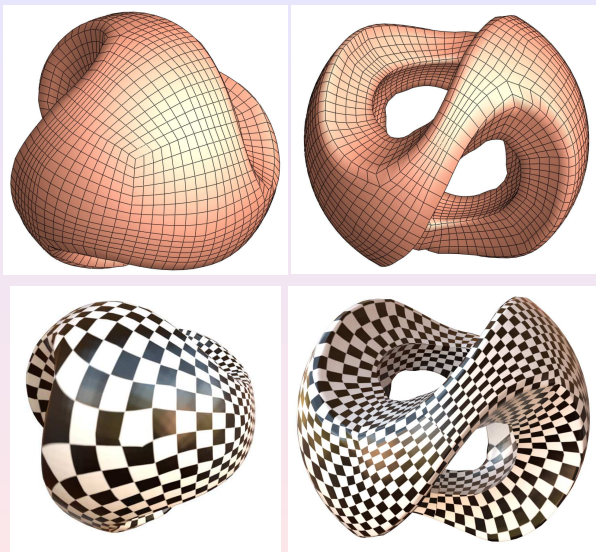


Figure: The genus 2 sculpt model.



Genus Two Case: Abel Condition

We set φ_0 as ω_0 and verify the Abel-Jacobi condition by computing the Abel-Jacobi map $\mu(D_Q - 4(\omega_0))$. The period matrix A of the Riemann surface S_Q is

$$\begin{pmatrix} 0.99999997 - i2.8e-09 & -0.24999994 + i2.745e-08 \\ 0.99999999 + i1.13e-08 & 0.50000015 + i4.1e-08 \end{pmatrix}.$$

The period matrix B is

$$\begin{pmatrix} -4.8789098e-19 + i0.50669566 & 7.5894152e-19 + i0.15720634 \\ -7.5894152e-19 + i0.73261918 & 4.8789098e-19 + i0.589281 \end{pmatrix}.$$

The Abel-Jacobi map image of the divisor is

$$\mu(D_Q - 4(\omega_0)) = \begin{pmatrix} -1.568599999979e-05 + i3.69999999994e-06 \\ 4.28899999998e-05 - i4.400000000182e-07 \end{pmatrix},$$

which is very close the 0.

Trinity Theorem

Colorable Quad-Mesh

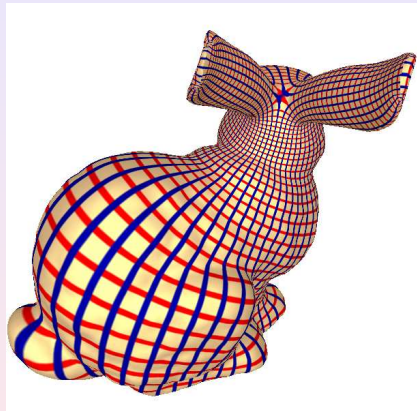
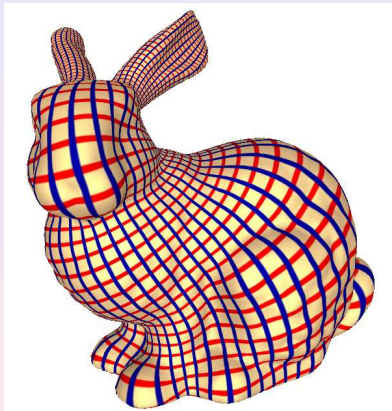
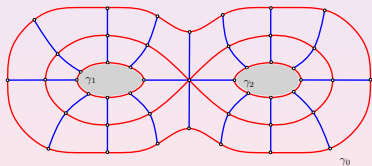


Figure: A red-blue (colorable) Quad-Mesh.

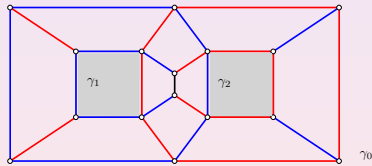
Colorable Quad-Mesh

Definition (Colorable Quad Mesh)

Suppose Q is a quadrilateral mesh on a surface S , if there is a coloring scheme $\iota : E \rightarrow \{\text{red}, \text{blue}\}$, which colors each edge either red or blue, such that each quadrilateral face includes two opposite red edges and two opposite blue edges, then Q is called a colorable (red-blue) quadrilateral mesh.



(a) Colorable quad-mesh.



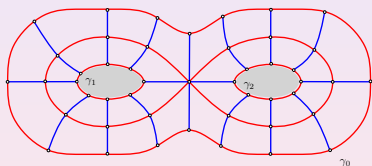
(b) Non-colorable quad-mesh

Figure: Quadrilateral meshes of a multiply connected planar domain.

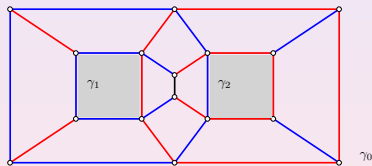
Colorable Quad-Mesh

Lemma

Suppose S is an oriented closed surface, \mathcal{Q} is a quadrilateral mesh on S . \mathcal{Q} is colorable if and only if the valences of all vertices are even.



(a) Colorable quad-mesh.



(b) Non-colorable quad-mesh

Figure: Quadrilateral meshes of a multiply connected planar domain.

Theorem (Trinity)

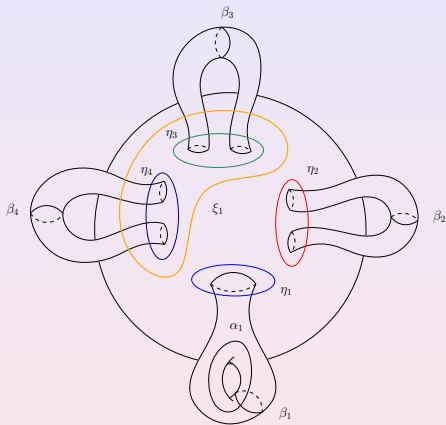
Suppose S is a closed Riemann surface with a genus greater than 1. Given an colorable quad-mesh \mathcal{Q} , there is a finite measured foliation $(\mathcal{F}_{\mathcal{Q}}, \mu_{\mathcal{Q}})$ induced by \mathcal{Q} , and there exists a unique Strebel differential Φ , such that the horizontal measured foliation induced by Φ , $(\mathcal{F}_{\Phi}, \mu_{\Phi})$ is equivalent to $(\mathcal{F}_{\mathcal{Q}}, \mu_{\mathcal{Q}})$. Inversely, given a Strebel differential Φ , it is associated with a finite measured foliation $(\mathcal{F}_{\Phi}, \mu_{\Phi})$, and induces a colorable quad-mesh \mathcal{Q} .

$\{\text{Colorable Quad-Mesh}\} \leftrightarrow \{\text{Finite Measured Foliation}\} \leftrightarrow \{\text{Strebel Differential}\}.$

Theorem

Suppose S is a compact Riemann surface embedded in \mathbb{R}^3 , the interior solid \mathcal{I} is a handle-body, then there exists a Strebel differential Φ , such that Φ induces a colorable quad-mesh \mathcal{Q}_Φ , \mathcal{Q}_Φ admits a hexahedral mesh of the enclosed volume \mathcal{I} of S .

Admissible Curve System



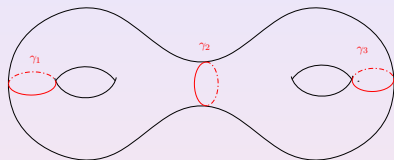
- 1 Boundaries of cutting disks β_k , $k = 1, \dots, g$
- 2 $\eta_k = \alpha_k \beta_k \alpha_k^{-1} \beta_k^{-1}$, $k = 1, \dots, g$
- 3 ξ_k , $k = 1, \dots, g-3$

We obtain an admissible curve system:

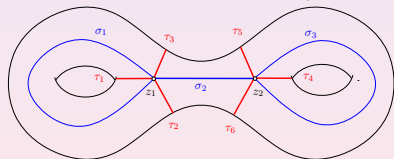
$$\Gamma = \{\beta_i, \eta_j, \xi_k\}$$

Figure: Admissible curve system.

Strebel Differential



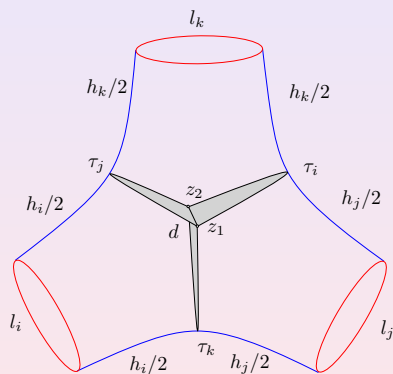
(a) Admissible curve system



(b) Colorable quad-mesh \mathcal{Q}_Φ

- 1 Admissible curve system Γ
- 2 The pants decomposition graph G_Γ with a height function h , determines a Strebel differential Φ
- 3 Zeros of Φ are z_1, z_2
- 4 Critical graph of Φ , $\{\tau_1, \tau_2, \tau_3, \tau_4, \tau_5, \tau_6\}$
- 5 Critical vertical trajectories $\{\sigma_k\}$, $k = 1, 2, \dots, 6g - 6$

Segmentation

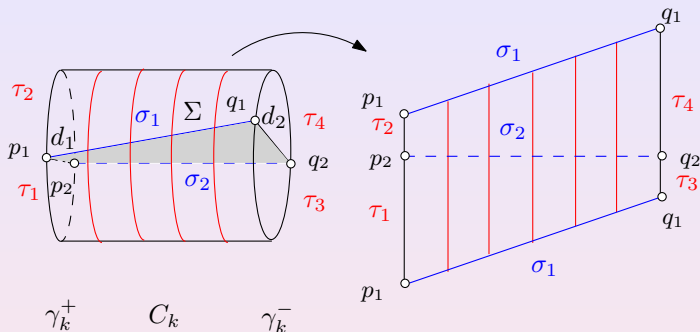


At each connected component of the critical graph $\{\tau_i, \tau_j, \tau_k\}$, the singular line d connects z_1 and z_2 , form 3 half-cutting-disks $\{D_i, D_j, D_k\}$,

$$\partial D_i = \tau_i \cup d$$

segment the interior volume into solid cylinders.

Segmentation

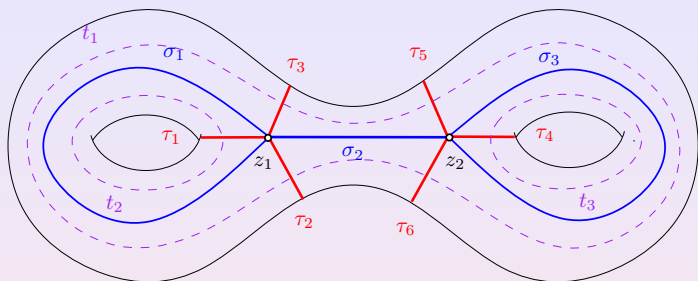


For each solid cylinder, construct a surface Σ ,

$$\partial\Sigma = \sigma_1 \cup \sigma_2 \cup d_1 \cup d_2,$$

the solid cylinder is divided into two half solid cylinders.

Segmentation



- The vertical STC chords of \mathcal{Q}_ϕ is shown as $\{t_1, t_2, t_3\}$, each chord represents a loop of half-solid-cylinders.
- Each loop of half-solid-cylinder is a direct product

$$D \times \mathbb{S}^1, \quad \partial D = \tau_k \cup d.$$

where D is a half disk.

- By “sweeping” method, one can generate the hexahedral mesh for each loop of half-solid-cylinders.

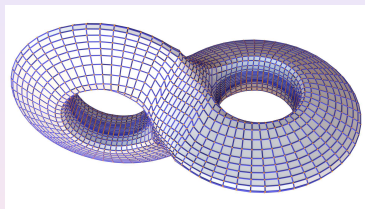
Strebel Differential to Quad-Mesh



(a)



(b)



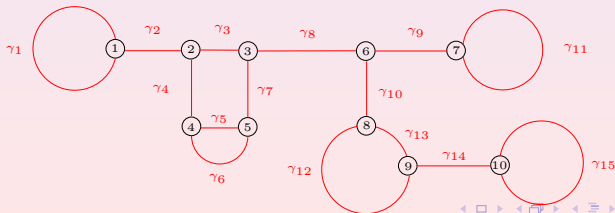
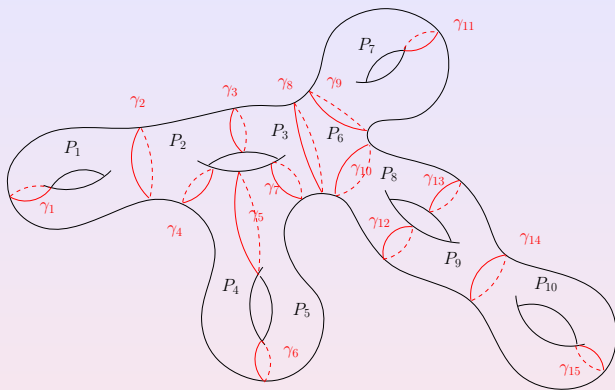
(c)

Figure: A Strebel differential on a genus two surface (a) and (b) induces a quad meshing (c).

Computational Algorithms

Algorithm for Computing Strebel Differential

Pants Decomposition



Pants Decomposition

Definition (Pants Decomposition)

Given a genus $g > 1$ closed surface S , a set of $3g - 3$ disjoint simple loops, $\Gamma = \{\gamma_1, \gamma_2, \dots, \gamma_{3g-3}\}$ is called an *admissible curve system*. Γ segments S into $2g - 2$ pairs of pants, $\{P_1, P_2, \dots, P_{2g-2}\}$, this forms a *pants decomposition* of the surface.

Definition (Pants Decomposition Graph)

- Each pair of pants is represented as a node.
- Each simple loop is denoted by an edge. Suppose the simple loop γ_i connecting two pairs of pants P_j, P_k , then the arc of γ_i connects nodes of P_j and P_k . G is called the *pants decomposition graph*.

Theorem (Hubbard and Masur)

Given non-intersecting simple loops $\Gamma = \{\gamma_1, \gamma_2, \dots, \gamma_{3g-3}\}$, and positive numbers $\{h_1, h_2, \dots, h_{3g-3}\}$, there exists a unique holomorphic quadratic differential Φ , satisfying the following :

- 1 The critical graph of Φ partition the surface into $3g - 3$ cylinders, $\{C_1, C_2, \dots, C_{3g-3}\}$, such that γ_k is the generator of C_k ,*
- 2 The height of each cylinder $(C_k, |\Phi|)$ equals to h_k , $k = 1, 2, \dots, 3g - 3$.*

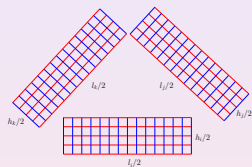
Poly-cylinder Surface

Given a Riemann surface S with genus $g > 1$, Φ is a Strebel differential, then the natural coordinates of $\Phi \zeta : U \rightarrow \mathbb{C}$ induces a flat metric with cone singularities, denoted as $|\Phi|$,

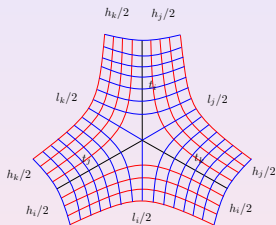
- 1 The zeros of Φ become cone singularities, with cone angle 3π ,
- 2 The critical graph of Φ partitions the surface into cylinders $\{C_1, C_2, \dots, C_{3g-3}\}$, the generators of the cylinders are $\Gamma = \{\gamma_1, \gamma_2, \dots, \gamma_{3g-3}\}$,
- 3 The pants decomposition graph induced by Γ is denoted as G_Γ ,
- 4 The heights of cylinder $(C_k, |\Phi|)$ is h_k ,
- 5 The circumference of $(C_k, |\Phi|)$ is l_k ,
- 6 The twisting angle of C_k is θ_k ,

then $(S, |\Phi|)$ can be represented by $(G_\Gamma, \mathbf{h}, \mathbf{l}, \theta)$.

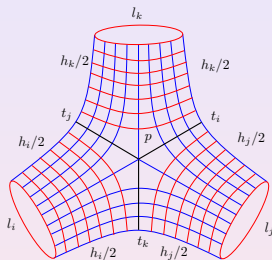
Poly-cylinder Surface



(a) 3 rectangles
 $l_j + l_k > l_i$



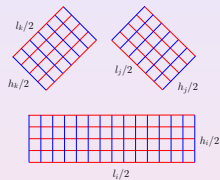
(c) a hexagon



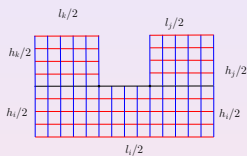
(e) a pair of pants
(type I)

Figure: Flat cylindric surface model of $(S, |\Phi|)$.

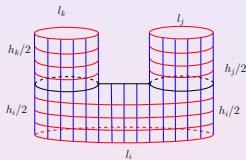
Poly-cylinder Surface



(a) 3 rectangles
 $l_j + l_k < l_i$



(b) a hexagon



(f) a pair of pants
(type II)

Figure: Flat cylindric surface model of $(S, |\Phi|)$.

Poly-cylinder Surface

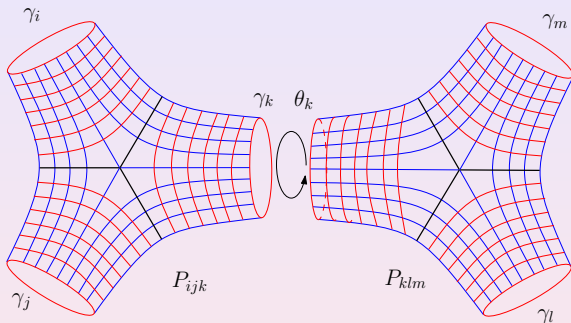
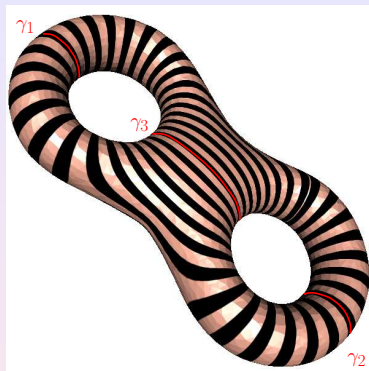


Figure: The twisting angle when gluing two pairs of pants.

Strebel Differentials



(a)



(b)

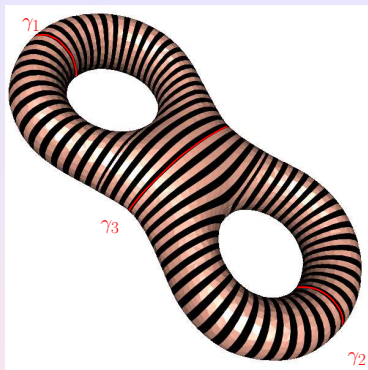
Figure: Strebel differentials on the genus two surface.

In the poly-cylinder surface model $(G_\Gamma, \mathbf{h}, \mathbf{l}, \theta)$, (\mathbf{l}, θ) give a local coordinates of the Teichmüller space. The height function \mathbf{h} changes.

Strebel Differentials



(c)



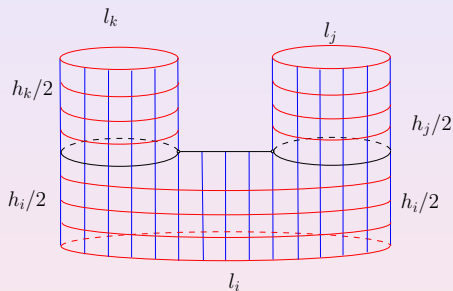
(d)

Figure: Strebel differentials on the genus two surface.

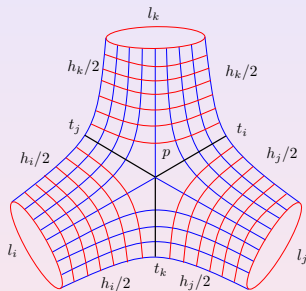
In the poly-cylinder surface model $(G_\Gamma, \mathbf{h}, \mathbf{l}, \theta)$, (\mathbf{l}, θ) give a local coordinates of the Teichmüller space. The height function \mathbf{h} changes.

Differential to Quad-Mesh

Given a Strebel differential Φ , we obtain a poly-cylinder surface,



(a) type II



(b) type I

Figure: Change each pair of pants of type II to that of type I by a Whitehead move.

Differential to Quad-Mesh

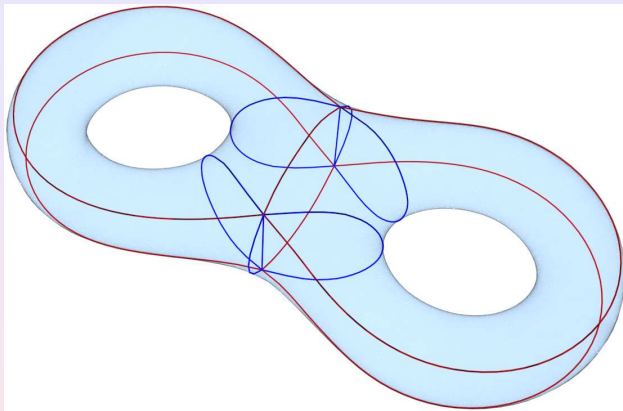


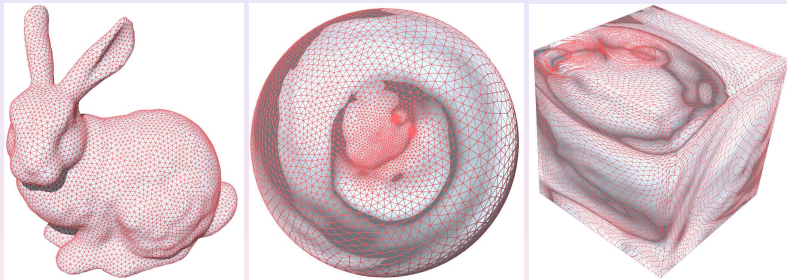
Figure: Divide each cylinder to two rectangles by connecting corresponding zeros on different boundary components; Construct an initial colorable quad-mesh;Subdivide.

Lemma

Suppose Φ is a Strebel differential on a compact Riemann surface S with genus greater than 0, then Φ induces a colorable (red-blue) quadrilateral mesh \mathcal{Q}_Φ of S .

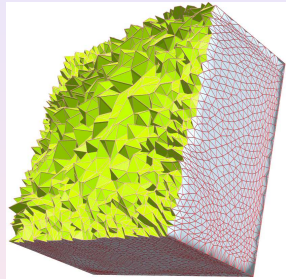
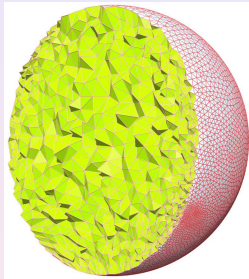
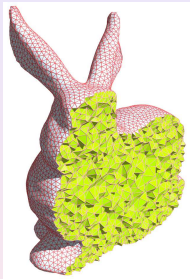
Algorithm for Hexahedral Meshing

Genus Zero Case



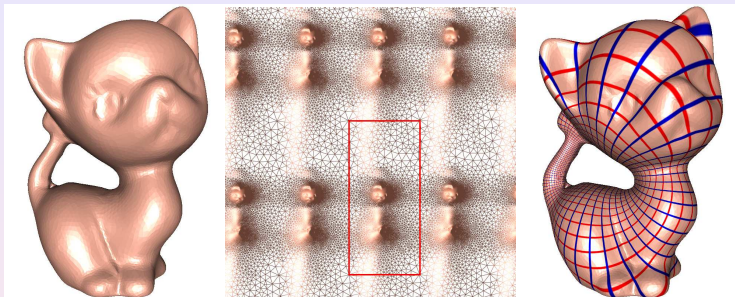
(a) Stanford bunny (b) Spherical mapping (c) Cube mapping

Genus Zero Case



(d) Solid bunny (e) Solid ball mapping (f) Solid cube mapping

Genus One Case



(a) Kitten surface

(b) Flat torus

(c) Quad-mesh

Figure: A genus one closed surface can be conformally and periodically mapped onto the plane, each fundamental domain is a parallelogram. The subdivision of the parallelogram induces a quad-mesh of the surface.

Genus One Case

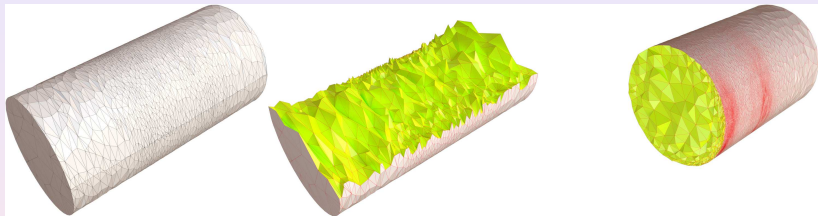


Figure: The interior of the kitten surface is mapped onto a canonical solid cylinder.

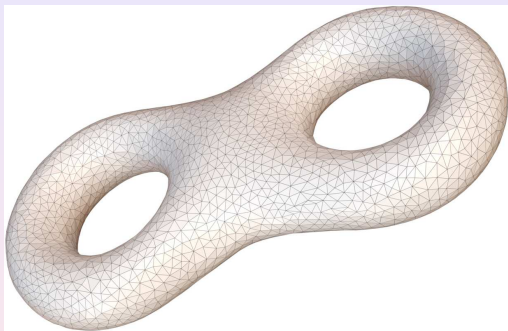


Figure: Input Surface.

Algorithmic Pipeline

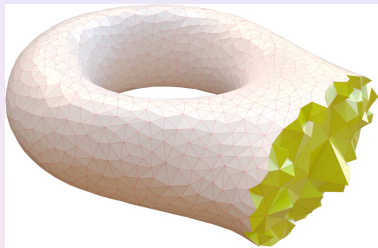


Figure: Tetrahedral meshing.

Algorithmic Pipeline

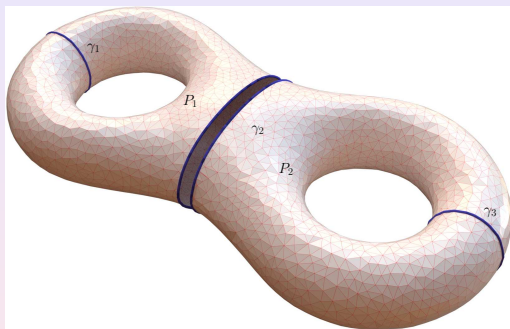


Figure: Admissible curve system, pants decomposition.

Algorithmic Pipeline

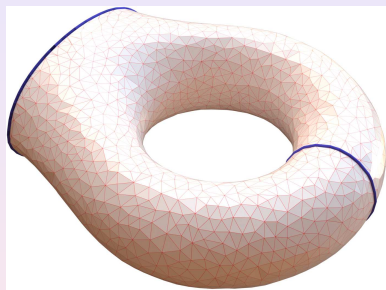
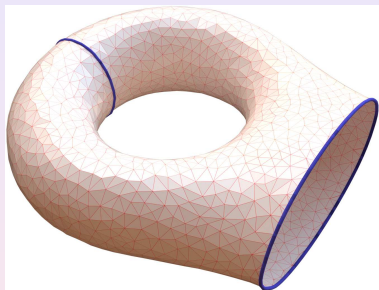


Figure: Two pairs of pants.

Algorithmic Pipeline

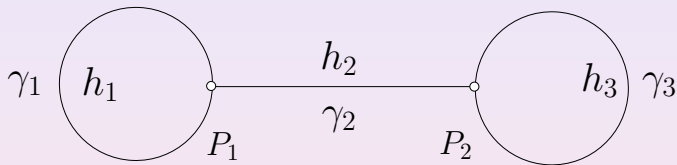


Figure: Pants decomposition graph.

Strebel Differentials



Figure: Holomorphic quadratic differential.

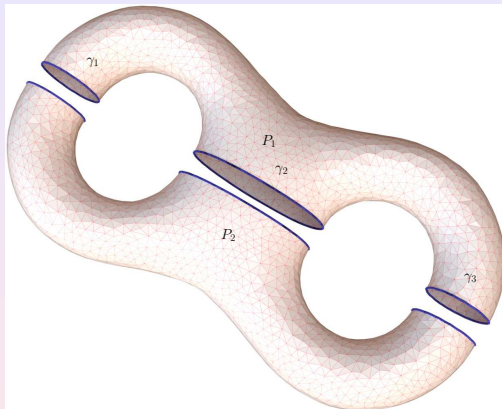


Figure: Admissible curve system, pants decomposition.

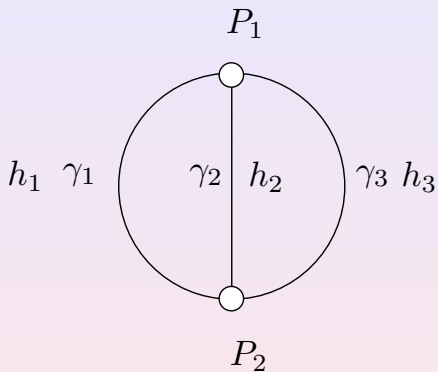


Figure: Pants decomposition graph.



Figure: Holomorphic quadratic differential.

Algorithmic Pipeline

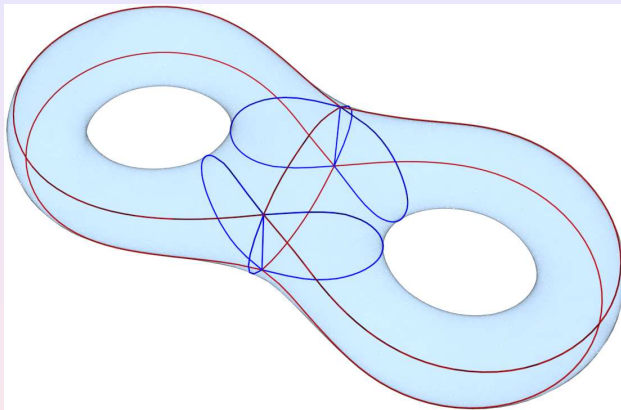


Figure: Critical horizontal trajectories and vertical trajectories.

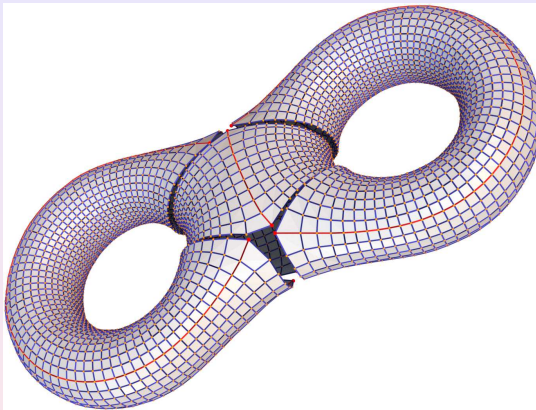


Figure: Cylindrical decomposition.

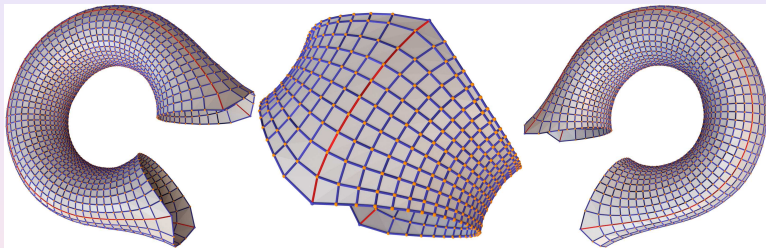


Figure: Cylindrical decomposition.

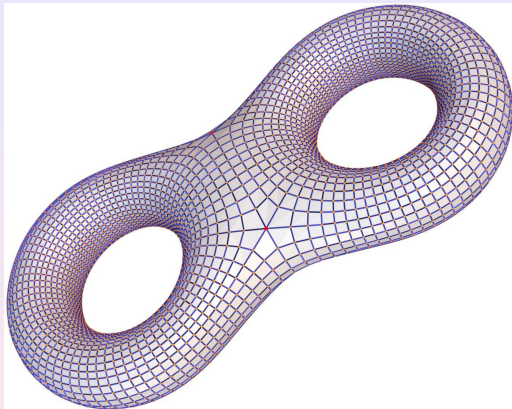


Figure: Colorable quadrilateral mesh.

Algorithmic Pipeline

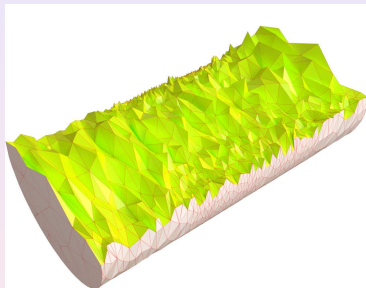
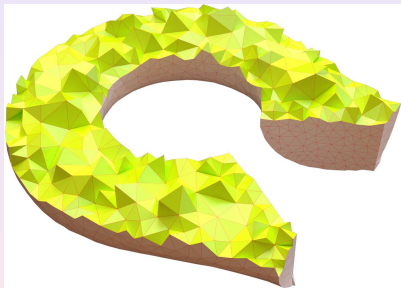


Figure: Left solid cylinder, maps to the canonical solid cylinder.

Algorithmic Pipeline

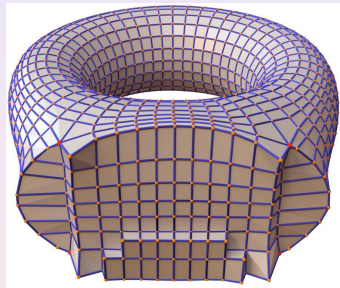
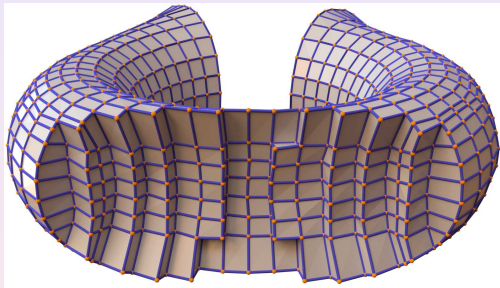


Figure: Hexahedral meshing of solid cylinders.

Algorithmic Pipeline

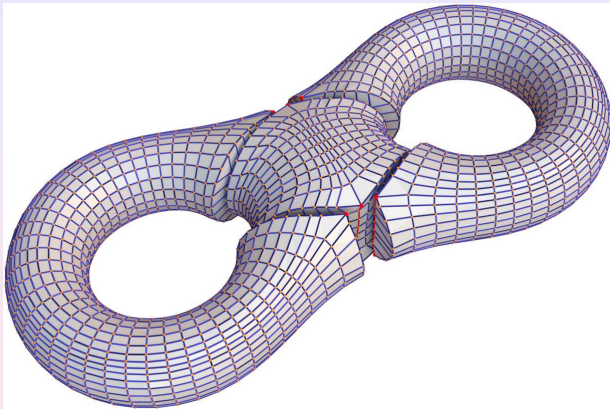


Figure: Hexahedral meshing of the interior volume.

Algorithmic Pipeline

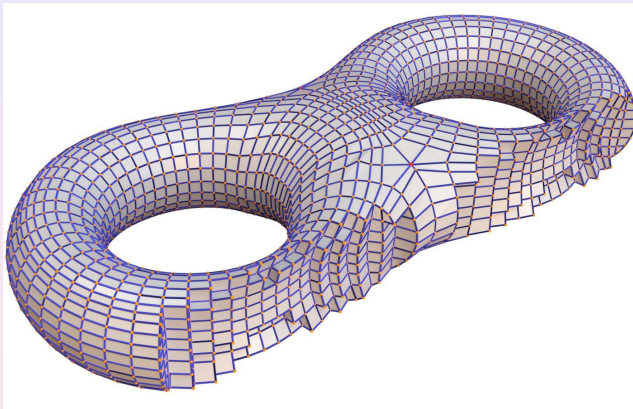


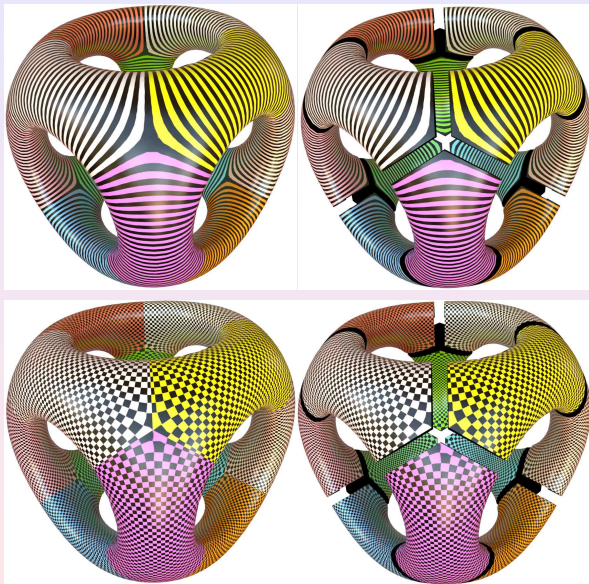
Figure: Hexahedral meshing of the interior volume.

Experimental Results

Experiments

The algorithm has been tested synthetic surfaces, surfaces scanned from real life, surfaces from mechanical CAD design and reconstructed from medical images. The algorithm is implemented using generic C++, the numerical computation is based on Eigen library. All our experiments are performed on a desktop computer with Intel(R) Core(TM) i7-4770 3.4GHz CPU and 16GB RAM.

Foliations



Foliations

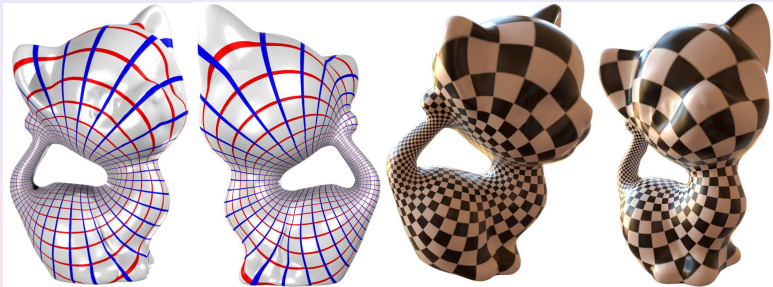


Figure: Conjugate foliations on a genus one surface.



Figure: Conjugate foliations on a facial surface.

Foliations



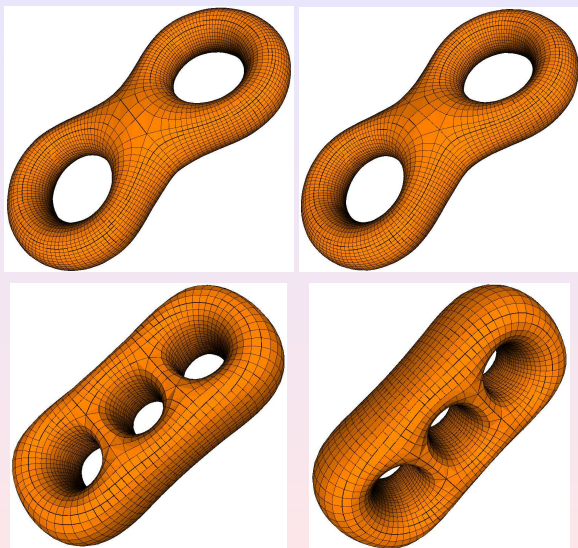


Figure: Quadrilateral meshes for genus two and three models

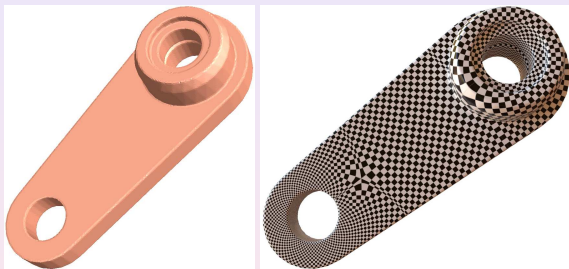


Figure: Conjugate foliations on a genus 2 mechanical part surface.

Foliations

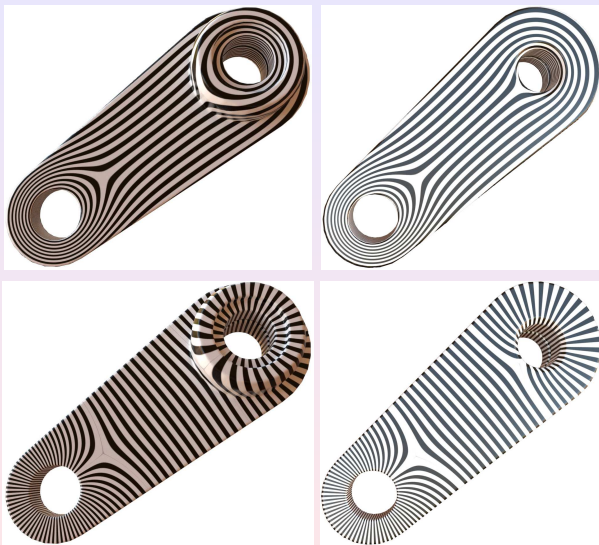


Figure: Conjugate foliations on a genus 2 mechanical part surface.

Quad-Mesh

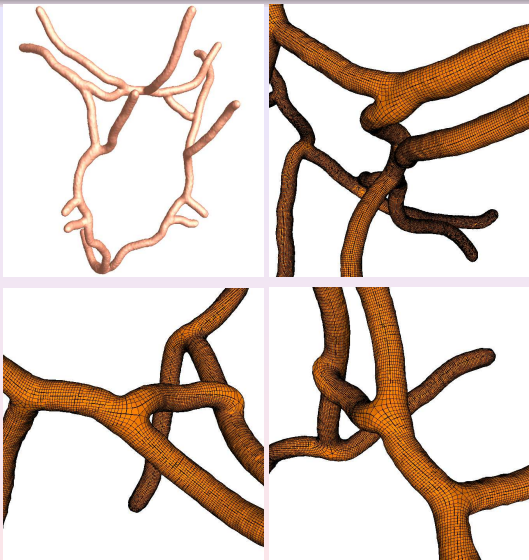


Figure: Quadrilateral mesh for the blood vessel model.

Genus Three Model

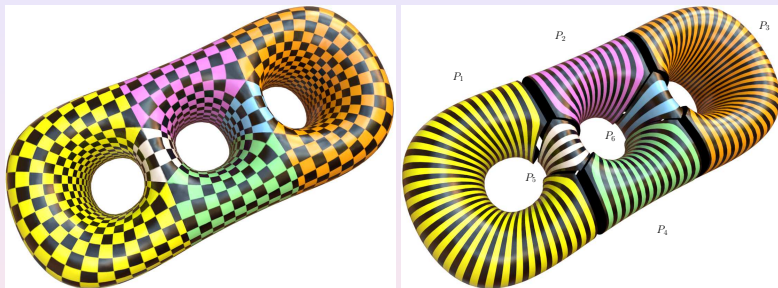


Figure: Holomorphic quadratic differential of a genus three surface.

Genus Three Model

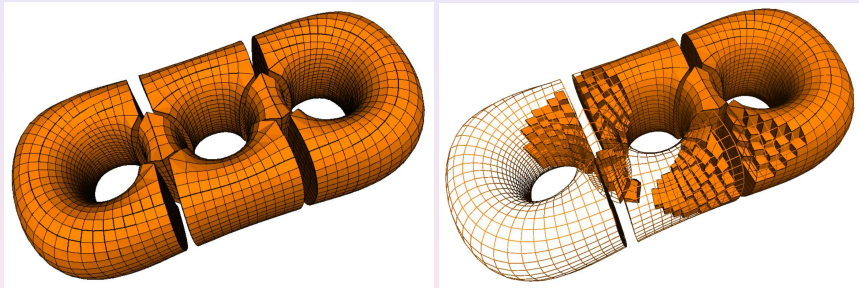


Figure: Hexahedral mesh of a genus three model.

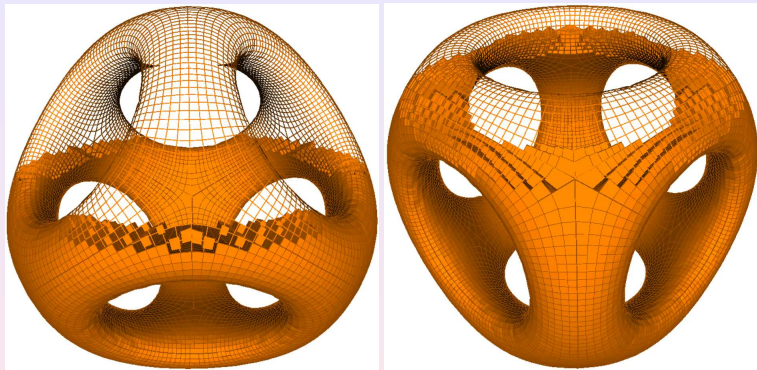


Figure: Hexahedral mesh of decocube model.

Computation Time

Model	# verts	# faces	genus	Bnd	Time(ms)
Alex face	80598	160058	0	1	2274
Cat	27894	55712	0	2	578907
Kitten	10000	20000	1	0	135823
Blood vessel	72312	144620	1	12	565012
Eight	3776	7556	2	0	32561
Nut	29840	59684	2	0	267234
3-hole torus	5996	12000	3	0	15142
Deco-cube	7492	15000	5	0	10008
Star cup	31029	62062	2	0	131114

Table: The computation time of foliations of different models.

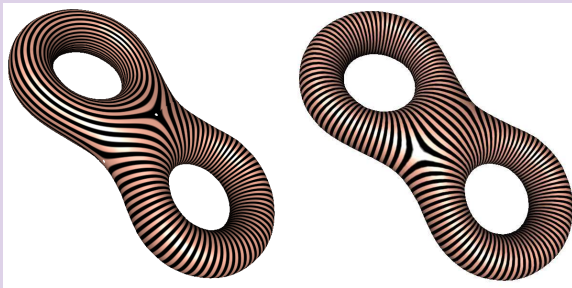
Conclusion

- 1 The quad-mesh metric satisfies conditions: Guass-Bonnet, holonomy, boundary alignment and finite geodesic lamination;
- 2 Equivalence between meromorphic quadratic differentials and quadrilateral meshes;
- 3 Singularities of a quad-mesh correspond to the divisor of the differential, which satisfies the Abel condition;
- 4 Colorable quad-mesh, measured foliations and Strebel differentials are equivalent;
- 5 Strebel differentials induce hexahedral meshes.

In the future, we will explore further along foliation mesh generation approach, to find feasible way to improve the uniformity of the cell sizes and the sharp feature alignment.

Thanks

For more information, please email to gu@cs.stonybrook.edu.



Thank you!